Energy Conversion and Management 80 (2014) 598–608

Contents lists available at ScienceDirect

Energy Conversion and Management

journal homepage: www.elsevier.com/locate/enconman

A technical and financial analysis of two recuperated, reciprocating engine driven power plants. Part 1: Thermodynamic analysis

Pedro Jose Orbaiz *, Michael J. Brear

Department Of Mechanical Engineering, University of Melbourne, Australia

ARTICLE INFO

Article history:
Available online 27 December 2013

Keywords:
Engine
Hybrid
Chemical recuperation
Natural gas
Biomass
Concentrated solar thermal

ABSTRACT

This paper is the first of a two part study that analyses the technical and financial performance of particular, recuperated engine systems. This first paper presents a thermodynamic study of two systems. The first system involves the chemical recuperation of a reciprocating, spark ignited, internal combustion engine using only the waste heat of the engine to power a steam–methane reformer. The performance of this system is evaluated for different coolant loads and steam–methane ratios. The second system is a so-called 'hybrid' in which not only the waste heat of the engine is used, but also a secondary heat source – the combustion of biomass. The effects of the reformer's temperature and the steam–methane ratio on the system performance are analysed.

These analyses show that the potential efficiency improvement obtained when using only the engine waste heat to power the recuperation is marginal. However, results for the hybrid show that although the overall efficiency of the plant, defined in terms of the energy from both the methane and biomass, is similar to that of the conventional, methane fuelled engine, the efficiency of the conversion of the biomass fuel energy to work output appears to be higher than for other biomass fuelled technologies currently in use. Further, in the ideal limit of a fully renewable biomass fuel, the burning of biomass does not contribute to the net CO_2 emissions, and the CO_2 emission reduction for this second plant can be considerable. Indeed, its implementation on larger internal combustion engine power plants, which have efficiencies of around 45–50%, could result in CO_2 emissions that are as much as 10–20% lower than typical natural gas combined cycle (NGCC) power stations. This appears to be a significant result, since NGCCs are commonly considered to have the lowest CO_2 emissions of all forms of fossil fuelled, power generation currently in use.

1. Introduction

As the world's energy demand grows, reducing greenhouse gas emissions to avoid the extreme climate change scenarios poses a significant challenge. While fossil fuel based technologies are relatively cheap and reliable, their higher greenhouse gas emissions are undesirable. On the other hand, baseload generation requirements and cost pose challenges for most renewable technologies. The integration of both fossil fuel and renewable energy sources may therefore be a viable way to reduce greenhouse gas emissions significantly in a cost-effective manner.

Hybrid cycles use both fossil and renewable energy inputs. This combination can reduce the overall carbon intensity of the plant, whilst maintaining the capacity factor and despachability of a fossil fuel plant. This approach may also improve the economics of the renewable technology [1–5]. Hybrid systems in the literature include integrated solar gas turbine combined cycles (natural gas and gasified coal) [2,3,5,6], co-fired coal and biomass [7], biomass assisted combined cycle gas turbines [4,1], amongst others.

Techno-economic evaluations of different power systems are used to evaluate the potential viability of a given technology, e.g. [8–11], throughout the first part of this research the technical performance of two chemically recuperated engine systems is analysed. This is done by undertaking a thermodynamic study of both cycles using the program ASPEN+ [12]. The first system involves the chemical recuperation of a spark ignited internal combustion engine (ICE) using only the waste heat of the engine to power a steam–methane reformer. The second simulation examines a hybrid cycle in which not only the waste heat of the engine is used, but also a secondary heat source is used to boost the steam–methane reforming process.

Steam–methane reforming is a well known process, with around 85% of the world's hydrogen produced using this method [13–17]. It is achieved by mixing steam and methane in the presence of a catalyst to obtain hydrogen and different products consisting of carbon, hydrogen and oxygen. At equilibrium, the

* Corresponding author.
E-mail addresses: pjorbaiz@unimelb.edu.au (P.J. Orbaiz), mjbrear@unimelb.edu.au (M.J. Brear).

0196-8904/$ - see front matter Crown Copyright © 2013 Published by Elsevier Ltd. All rights reserved.
http://dx.doi.org/10.1016/j.enconman.2013.11.051

extent to which the reactions are shifted towards the products or the reactants depends on the reactant quantities and the temperature and pressure at which the reaction takes place, and also the assistance of a catalyst [18–21]. Industrial applications usually use nickel based catalysts which operate at around 700 °C and above [14,16,22,23].

Chemically recuperating a thermo-mechanical power unit is not a new idea, e.g. [24]. Rostrup-Nielsen [25] analyses the different uses of chemical recuperation, not only in power generation, but also in the industrial production of hydrogen, ammonia, methanol and syngas for gas-to-liquid plants. A relatively large amount of work has been published on chemical recuperation of gas turbines [24–31]. However, no power plants based on this concept appear to have been built.

Integrating steam methane reformers (SMRs) with internal combustion engines (ICEs) has received less attention than gas turbines. However, in the last decade in particular, the concept has gained interest in the research community [32–36]. Work done on the chemical recuperation of natural gas fuelled internal combustion engines shows that while the degree of recuperation is lower than for gas turbines, other benefits are obtained by its implementation. Due to the combination of the combustion properties of methane, carbon monoxide and hydrogen, the synthesis gas resulting from the reforming reaction has several enhanced combustion properties [34,37–44]. These include hydrogen having broad flammability limits, low activation energy and high flame velocity, allowing synthesis gas fuelled engines to run leaner. This can significantly improve the engine efficiency and reduce pollutant emissions if implemented properly.

However, the relatively low exhaust temperature of internal combustion engines nonetheless remains as a significant issue, prompting this work's proposed use of a secondary renewable energy source to raise the reforming temperature. The relative performance of these cycles is demonstrated by first examining the basic, chemically recuperated cycle, and then examining an equivalent, hybrid cycle with the secondary, renewable energy source included. The second part of this two part study then considers the financial performance of hybrids only, since the thermodynamic benefit of the basic cycle is found to be marginal.

2. Cycle layout and description

Fig. 1 shows the layouts of the chemically recuperated cycles. The basic system is shown in Fig. 1a and is composed of 4 main streams. Stream 1 is the inlet air to the engine. Streams 2, 3, 4 and 5 are the engine exhaust gases after going through the engine, the SMR, the steam generator/methane super-heater and the condenser respectively. Stream C is the coolant flow of the engine; part of its heat is used to pre-heat the fuel and the water. The rest of the heat is dumped into the atmosphere through a radiator in order to achieve the cooling stream inlet temperature. Stream F is the fuel line and W is the water flow that goes into the SMR. Both lines are pre-heated with the coolant flow and then super-heated with the exhaust gases and consequently mixed before entering the reformer.

Fig. 1b shows the proposed layout for the hybrid. In this case, the heat from the exhaust gases and the cooling system are used to preheat the steam and methane, which is then reformed in a biomass fired SMR. Stream 1 is the inlet air to the engine, 2, 3 and 4 are the different paths of the exhaust gases as they go through the different heat exchangers. Stream C is the cooling flow of the ICE. Part of its heat is used to pre-heat the methane and the water; the rest is dumped into the atmosphere through a radiator in order to achieve the cooling stream inlet temperature. Line F carries the fuel and W is the water flow that goes into the reformer. Both lines are mixed and pre-heated with the cooling flow, and then super-heated with the engine exhaust gases in the steam generator and methane super-heater before entering the reformer. Line BM carries the air which passes through the biomass burner. Stream BIOMASS is the biomass intake of the combustor. The *LHV* of different biomass fuels ranges approximately between 15 and 25 MJ/kg [45–47], therefore it is reasonable to assume that the biomass used in this process has a *LHV* of 20 MJ/kg, although this dose not affect the cycle analysis. The heat from this process is used to maintain the temperature of the SMR output stream at a pre-set value.

Table 2 shows the pressure and temperature of the input streams of both cycles.

2.1. Steam–methane reformer (SMR)

In both Fig. 1a and b the steam–methane reformer is represented as block SMR. It is modelled as an adiabatic, equilibrium reactor. In the case of the chemically recuperated cycle, heat is extracted from the exhaust gases and dumped into the reformer to feed the endothermic steam–methane reforming reaction. In the case of the hybrid cycle the SMR is kept at a constant temperature using the heat of the biomass combustion.

Non-equilibrium effects are likely to make the process too slow at temperatures below 700 K [18–21]. Thus, 700 K is defined as the minimum catalyst activation temperature (MCAT). The MCAT is the temperature below which the catalyst is unlikely to be active and therefore chemical recuperation is not feasible. It is also relevant to define an industrial catalyst activation temperature (ICAT), which is the temperature at which most industrial catalyst start to work. This will be set at 1000 K [14,16,22,23]. Non-equilibrium membrane reformers would be ideal for this application, because of their high methane conversion factor (90%) at lower temperatures [48–52]. However, because such devices are still not commonly used and are in development, they will not be modelled in this research. The heat transfer effectiveness of the SMR is set at 80%.

Since lower pressure favours the reaction, the pressure in the reformer is set to the lowest at which proper injection of the fuel can be achieved. According to previous work done with a natural gas powered ICE [53,54], this is around 0.5 MPa, which will be the pressure used in the entire fuel line F.

2.2. Heat exchangers

Blocks H_2O-PH and CH_4-PH are counter current heat exchangers that use the hot water from the engine's coolant circuit to pre-heat the water and methane coming out of the pump and compressor respectively. The steam generator and methane super-heater, blocks STEAM-GN and CH_4-SH, are also counter current heat exchangers. It is during this stage where the water and methane are super-heated with the exhaust gases before entering the SMR. The effectiveness of the low and high temperature heat exchangers is 80% and 90% respectively.

Blocks RAD and COND work are a radiator and a condenser, respectively. They dump the excess heat of streams C and F into the atmosphere. In the case of the condenser, it is during this stage where the injected water and some of the water generated during the combustion can be recovered.

The Biomass burner consists of two parts. The BM-PH is the biomass burner air pre-heater. It recirculates the hot biomass exhaust gases coming out of the biomass combustor to pre-heat the biomass inlet air stream. Block BM-BURN is modelled as a combustor in which the biomass is burnt and the heat of the combustion is transferred to the SMR. The efficiency of the process, defined as

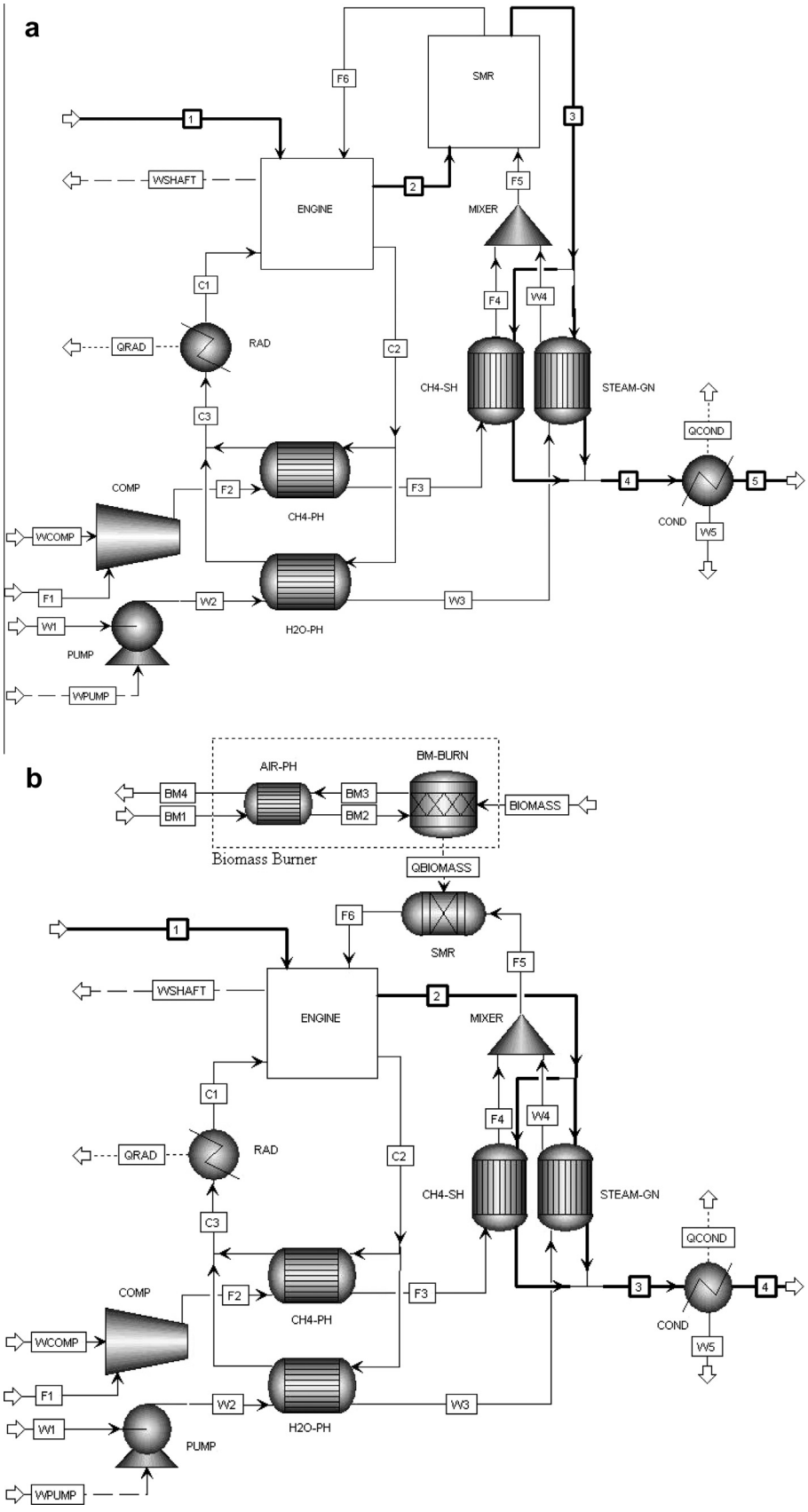

Fig. 1. Cycles layout. (a) ICE chemical recuperation. (b) Hybrid chemical recuperation.

Table 1
Hybrid cycle's operating conditions.

	Case 1	Case 2
Lambda (λ)	2	2
Steam–methane ratio	2	1
SMR temperature (K)	1200	900
Biomass heat transfer efficiency	85%	85%
SMR pressure (MPa)	0.5	0.5

Table 2
Composition, temperature and pressure of the different inlet streams.

Stream	Composition	Temperature (K)	Pressure (MPa)
1	Air	298	0.1
C1	Water	350	0.15
F1	Methane	298	0.1
W1	Water	298	0.1

the energy entering the SMR relative to that released by the biomass combustion, is assumed to be 85%.

2.3. Engine

The energy content of the input streams is split into shaft work, exhaust heat and cooling heat. The efficiency of the engine is kept constant at 40% (unless specified otherwise).

2.4. Pump, compressor and mixer

The pump is an adiabatic block with a 5:1 pressure ratio and an efficiency of 30%. The compressor is also adiabatic and has the same pressure ratio as the pump, but its efficiency is set at 80%. The mixer is modelled as an adiabatic process in which streams F and W are combined. No pressure drop has been imposed.

3. Simulation methodology

Previous work done on natural gas and hydrogen ICEs shows that the maximum efficiency of these two cycles is obtained when running between $\lambda = 1.5$ and $\lambda = 2.5$ [55–61]. In order to be consistent with this, and since syngas is a mixture containing methane and hydrogen, the simulations will be done with 100% excess air ($\lambda = 2$), where the efficiency should be maximised and further gains due to lean combustion are limited.

The engine waste heat (60% of the inlet stream's enthalpy) is split into the exhaust and cooling streams. Most engines normally dispose of roughly half of the waste heat through the cooling system and the other half as hot exhaust gases. However, in order to analyse the advantages of disposing of the waste heat as high grade heat (exhaust gas) rather than low grade heat (coolant stream), the chemically recuperated cycle is evaluated for different enthalpy splits between these two heat sinks. This will be referred to as the 'exhaust-coolant enthalpy split'. In the case of the hybrid system the performance and efficiency of the entire cycle is evaluated for different SMR temperatures. Also, the effects of the steam–methane ratio entering the SMR are analysed for both cycles.

4. Results and discussion

4.1. ICE chemical recuperation

Fig. 2 shows the temperature of the reforming reaction in the SMR for the different steam–methane ratios. It shows that the temperature drops as the amount of steam entering the SMR increases.

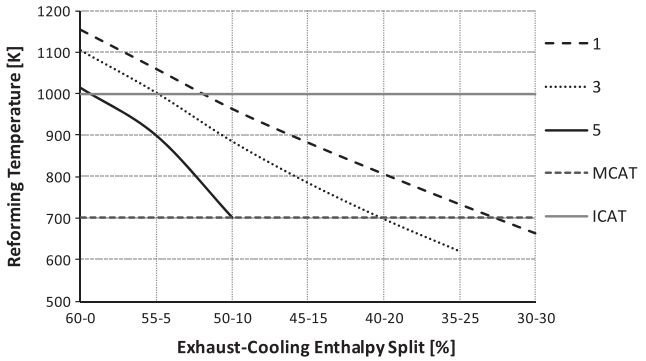

Fig. 2. SMR temperature versus exhaust-cooling enthalpy split for different steam/methane ratios (MCAT and ICAT stand for minimum catalyst activation temperature and industrial catalyst activation temperature respectively).

As expected, it also shows that the temperature of the reforming process increases as the enthalpy split tends towards 60% exhaust, 0% coolant (i.e. more like a gas turbine). As explained earlier, the MCAT is the minimum temperature at which the catalyst is considered to be active and the ICAT is the industrial catalyst activation temperature. Because it is considered that the reforming will not reach equilibrium for temperatures below the MCAT, operation below this temperature should be considered unlikely.

Fig. 3 shows the percentage of methane reformed as a function of the exhaust-cooling enthalpy split for the different steam–methane ratios. Comparing Figs. 2 and 3, it can be seen that while the temperature of the reaction is higher for a steam–methane ratio of 1, for all enthalpy splits, the methane conversion does not follow this trend. This is because increased steam–methane ratios also favour the reaction. However acting against this is the mixture's increased specific heat with increased steam content. Thus, an optimum steam–methane ratio exists that maximises methane conversion. In most cases, this optimum is roughly 3.

The overall efficiency of the system in Fig. 1a can be written as:

$$\eta = \frac{W - W_p - W_c}{N^{F1} LHV_{CH_4}} \quad (1)$$

where W, W_c and W_p are the engine, the compressor and the pump work respectively (kW), N^{F1} is the molar flow of stream $F1$ (kmole/s) and LHV_{CH_4} is the lower heating value of methane (kJ/kmole). Fig. 4 shows that the efficiency of the cycle increases with the steam–methane ratio as well as when the enthalpy shifts towards the 60-0 split. This, again, is because there is more enthalpy available in the exhaust and therefore higher reforming temperatures can be achieved, allowing a higher degree of reformation.

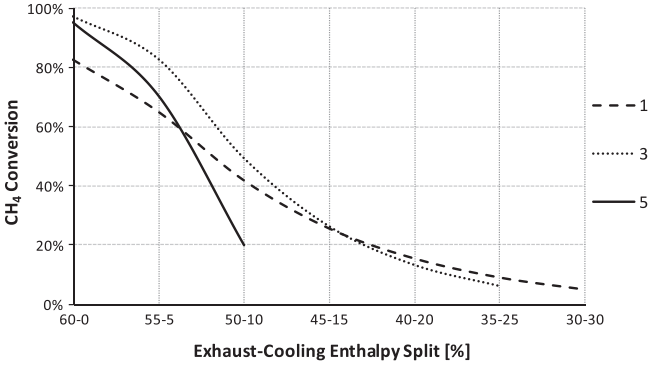

Fig. 3. CH_4 mass conversion percentage versus exhaust-cooling enthalpy split for different steam–methane ratios.

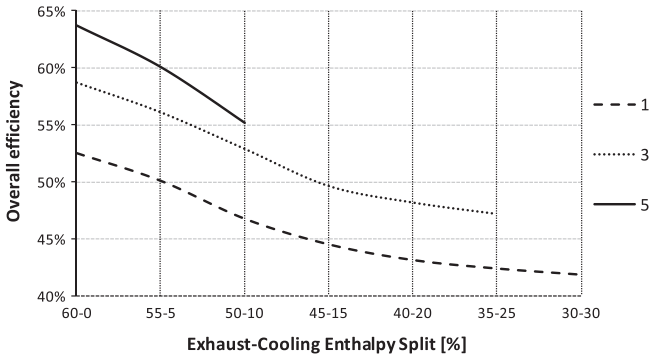

Fig. 4. Overall efficiency versus exhaust-cooling enthalpy split for different steam–methane ratios.

The engine work (W) in Eq. (1) can be written as

$$W = \eta_E \left[N^{F6} \left(X^{F6}_{CH_4} LHV_{CH_4} + X^{F6}_{H_2} LHV_{H_2} + X^{F6}_{CO} LHV_{CO} \right) + Q^{F6} \right], \quad (2)$$

where LHV_i is the lower heating value of the different reformed products (kJ/kmole), N^{F6} is the molar flow of stream $F6$ (kmole/s), X^{F6}_i is the molar fraction of the different combustible components in stream $F6$, η_E is the engine efficiency and Q^{F6} is the added sensible enthalpy of stream $F6$. It is noted that the engine needs to be direct injected or boosted to make use of this enthalpy. The term Q^{F6} can be written as

$$Q^{F6} = \sum \left(m_i h_{i,(T^{F6},P^{F6})} - m_i h_{i,(298\ K,1atm)} \right), \quad (3)$$

where m_i and h_i are the mass and specific enthalpy of the different reformed products, respectively. When η_E is defined in this way, it incorporates work production both by combustion and expansion of the steam in the mixture. If the increment in the LHV of the fuel due to reformation is

$$\Delta LHV_R = N^{F6} \left(X^{F6}_{CH_4} LHV_{CH_4} + X^{F6}_{H_2} LHV_{H_2} + X^{F6}_{CO} LHV_{CO} \right) - N^{F1} LHV_{CH_4}, \quad (4)$$

Then Eq. (1) can be rewritten as

$$W = \eta_E \left[\Delta LHV_R + N^{F1} LHV_{CH_4} + Q^{F6} \right]. \quad (5)$$

This means that the overall efficiency of the system (Eq. (1)) can be expressed as

$$\eta = \eta_R + \eta_E + \eta_H + \eta_{pc} \quad (6)$$

where

$$\eta_R = \frac{\eta_E \Delta LHV_R}{N^{F1} LHV_{CH_4}}, \ \eta_H = \frac{\eta_E Q^{F6}}{N^{F1} LHV_{CH_4}}, \ \eta_{pc} = -\frac{(W_p + W_c)}{N^{F1} LHV_{CH_4}}. \quad (7)$$

The terms η_R, η_H, and η_{pc} are respectively the efficiency contribution of reforming the fuel, the efficiency contribution of the added sensible enthalpy and the negative contribution caused by the work of the pump and the compressor.

Fig. 5 shows that while η_R drops as the enthalpy split is shifted towards the coolant stream, η_H remains practically constant, as long as the SMR temperature is above or close to the MCAT temperature. Past this point, both η_R and η_H drop. It is also clear that the rise of the overall efficiency when increasing the steam–methane ratio is mostly due to heat recovery rather than reforming. This is consistent with the data shown in Figs. 3 and 4. This shows that the so-called 'steam engine' effect can be significant. The negative contribution of η_{pc} is equal for all operating points and is approximately 1%.

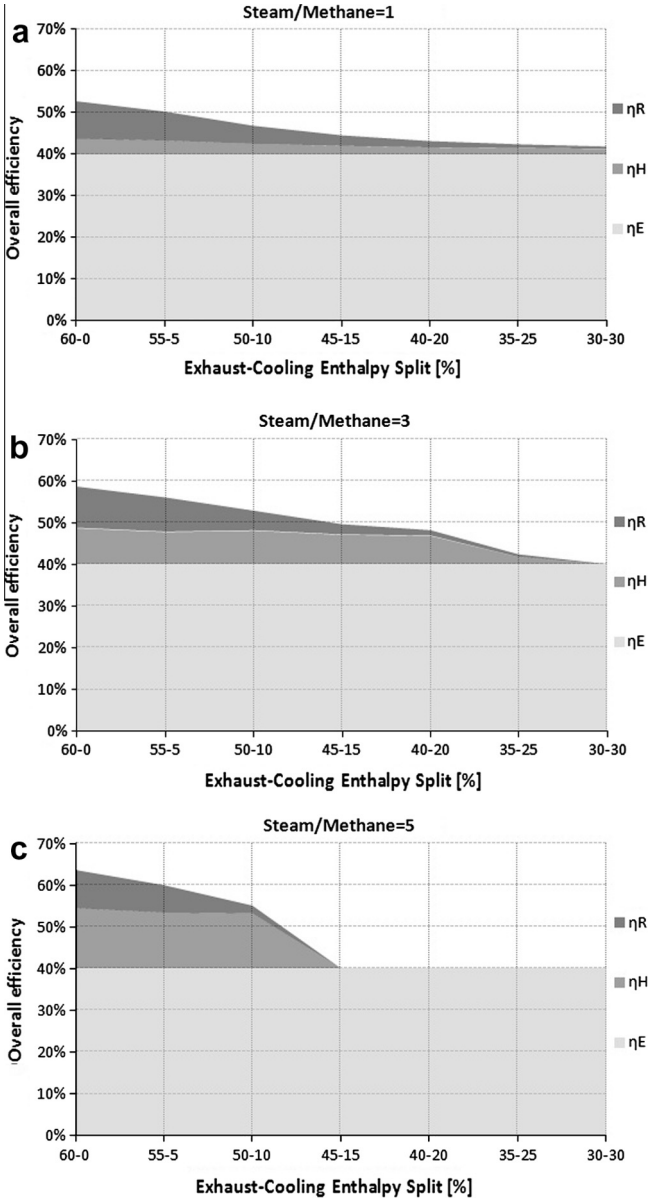

Fig. 5. Efficiency contributions due to heat and chemical recuperation, versus exhaust-cooling enthalpy split for different steam–methane ratios. (a) Steam–methane ratio = 1. (b) Steam–methane ratio = 3. (c) Steam–methane ratio = 5.

Figs. 2–5 also show that for conventional engines, which normally dispose of roughly half of their waste heat through the coolant stream and the other half as hot exhaust gases, chemical recuperation is unlikely as the reformer dose not achieve the MCAT (Fig. 2). Furthermore, even if 3/4 of the waste heat where to be disposed as high grade exhaust heat (45–15 exhaust-cooling enthalpy split) the efficiency improvements still require low temperature reforming, which is a significant practical challenge.

4.2. Hybrid ICE with chemical recuperation

As mentioned previously, the hybrid cycle incorporates a secondary, carbon neutral energy source to promote the reforming reaction. Fig. 6 shows the ratio of biomass–methane energy ratio versus steam–methane ratio for the different SMR temperatures. It shows that the biomass energy requirement increases to sustain a given SMR temperature as the steam–methane ratio increases.

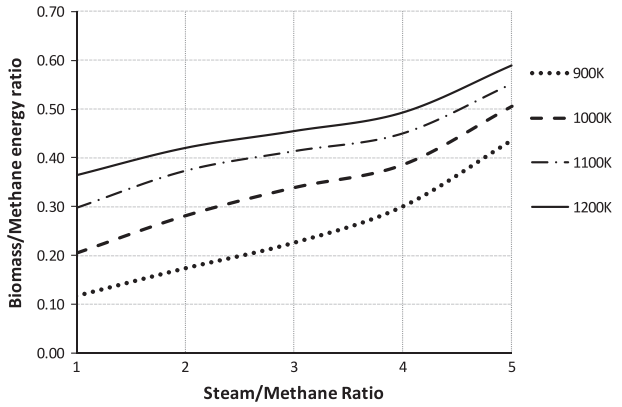

Fig. 6. Hybrid cycle energy input ratio of biomass–methane versus steam–methane ratio for the different SMR temperatures.

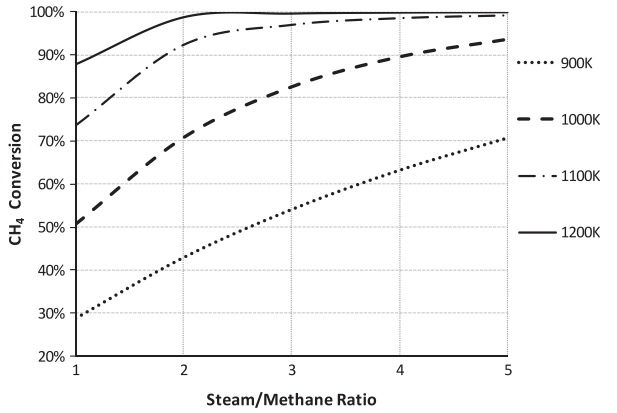

Fig. 7. Hybrid cycle methane conversion percentage versus steam–methane ratio, for different SMR temperatures.

Fig. 7 shows the percentage of methane reformed at the different operating conditions. As expected, the reforming reaction is favoured by high temperatures and high steam–methane ratios. It is also noted that for an SMR temperature of 1200 K the methane conversion is complete at a steam–methane ratio of 2 and therefore no further gains due to chemical recuperation are obtained beyond this point.

The overall efficiency of the hybrid cycle (Fig. 1b) can be defined as

$$\eta = \frac{W - W_p - W_c}{N^{F1} LHV_{CH_4} + N^{BM} LHV_{BM}} \tag{8}$$

where W, W_c and W_p are again the engine, the compressor and the pump work respectively (kW), LHV_{CH_4} and LHV_{BM} are the lower heating values of methane and biomass (kJ/kmole), and N^{F1} and N^{BM} are their molar flow rate (kmole/s). Fig. 8 shows that the overall cycle efficiency has an optimal steam–methane ratio for all four SMR temperatures. Beyond this optimum the energy needed to heat the excess water in the reactants up to the SMR's operating temperature is greater then the energy recovered. It can also be seen that the efficiency of the cycle is higher for intermediate steam–methane ratios with a reforming temperature of 900 K.

As in the previous section, the shaft work done by the system can be expressed by Eq. (5). Therefore, the overall efficiency of the system (Eq. (8)) is

$$\eta = \frac{\eta_E \left[\Delta LHV_R + N^{F1} LHV_{CH_4} + Q^{F6}\right] - W_p - W_c}{N^{F1} LHV_{CH_4} + N^{BM} LHV_{BM}}. \tag{9}$$

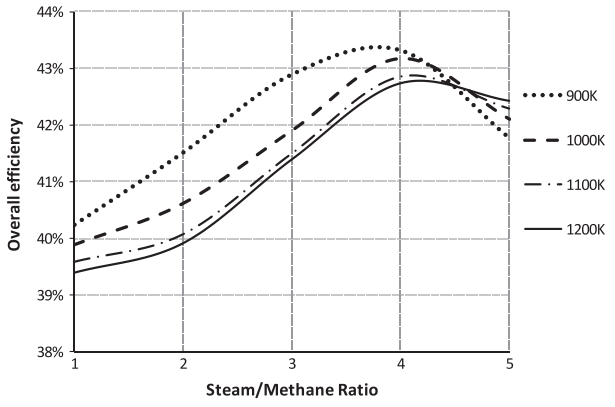

Fig. 8. Hybrid cycle overall efficiency versus steam–methane ratio, for different SMR temperatures.

Rearranging Eq. (9), the following efficiency contributions can be defined

$$\eta = \eta_R + \eta_{CH_4} + \eta_H + \eta_{pc}, \tag{10}$$

where

$$\eta_R = \frac{\eta_E \Delta LHV_R}{N^{F1} LHV_{CH_4} + N^{BM} LHV_{BM}}, \quad \eta_{CH_4} = \frac{\eta_E N^{F1} LHV_{CH_4}}{N^{F1} LHV_{CH_4} + N^{BM} LHV_{BM}},$$

$$\eta_H = \frac{\eta_E Q^{F6}}{N^{F1} LHV_{CH_4} + N^{BM} LHV_{BM}}, \quad \eta_{pc} = -\frac{(W_p + W_c)}{N^{F1} LHV_{CH_4} + N^{BM} LHV_{BM}}. \tag{11}$$

The terms $\eta_R, \eta_{CH_4}, \eta_{RH}$ and η_{pc} are respectively the efficiency contribution of reforming the fuel, the efficiency contribution of the methane, the efficiency contribution of the added sensible enthalpy and the negative contribution caused by the work of the pump and the compressor.

Fig. 9 shows that η_E decreases as the steam–methane ratio is increased in all cases. This is because of the extra energy required to heat the excess steam to the reformer temperature and also to feed the reforming reaction. However, this is counteracted by an increase of both η_R and η_H. Again, the negative contribution of η_{pc} is comparable for all operating points and is of order 1%.

Although the biomass heat input needs to be taken into account when calculating the cycle efficiency, it can be disregarded when calculating its CO_2 emissions. This is because the burning of biomass is assumed to not contribute to the net anthropogenic CO_2 emissions in the ideal limit of a fully renewable biomass fuel. Thus, the CO_2 emissions of the hybrid cycle can be calculated as

$$\frac{m_{CO_2}}{W_{net}} = \frac{N_{CO_2} M_{CO_2}}{W - W_c - W_p}, \tag{12}$$

where N_{CO_2} is the number of moles of CO_2 produced by the cycle per hour and M_{CO_2} is the molar weight of CO_2. Comparing Figs. 8 and 10 it can be seen that although the efficiency of the cycle has an optimum, the CO_2 emissions drop monotonically with steam–methane ratio and temperature.

Fig. 11 shows the CO_2 emission reduction percentage of the proposed hybrid cycle compared with a 40% efficient natural gas engine. It shows that the CO_2 reductions obtained by applying boosted chemical recuperation to a natural gas engine can vary from 11% to 41%, depending on the cycle operation conditions.

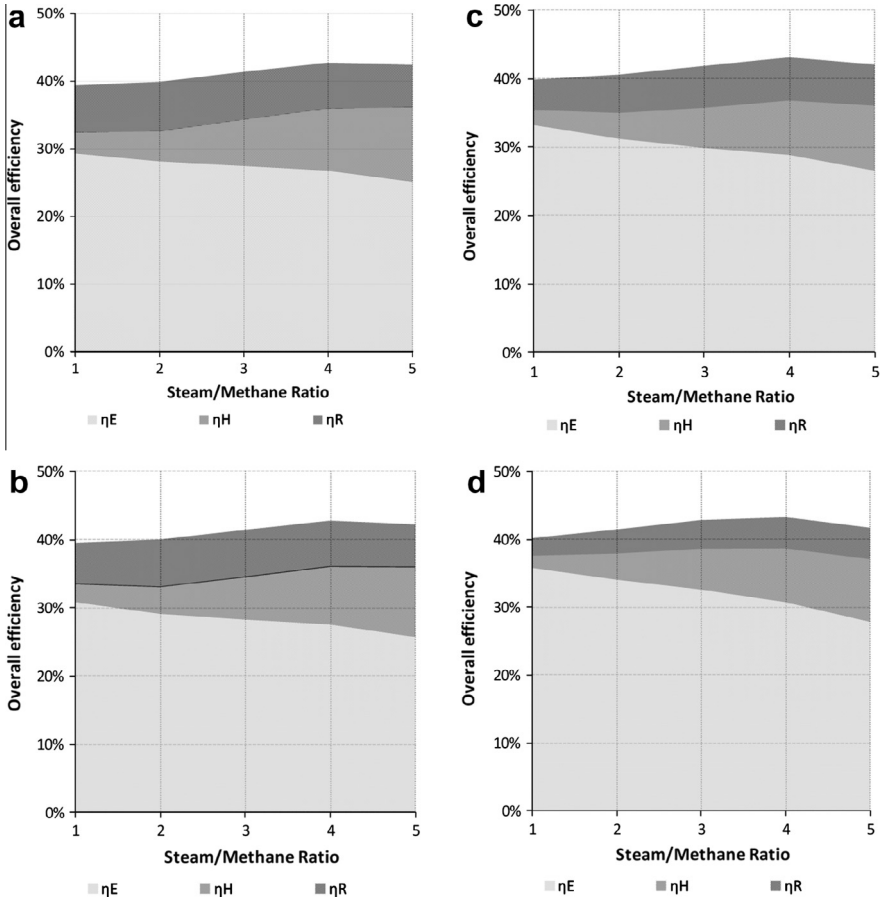

Fig. 9. Hybrid cycle efficiency contributions of the engine and biomass burner, heat and chemical recuperation, versus steam/methane ratio for different SMR temperatures. (a) 1200 K. (b) 1100 K. (c) 1000 K. (d) 900 K.

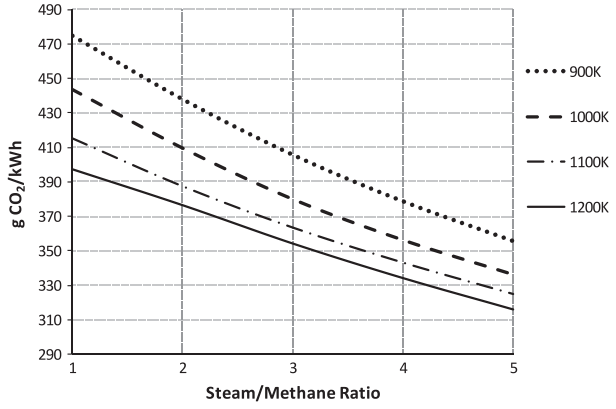

Fig. 10. Hybrid cycle CO_2 emissions versus steam–methane ratio, for different SMR temperatures.

4.2.1. Comparison with other biomass fuelled power plants

In order to justify the integration of the biomass burner it is important to quantify the benefit gained by using the biomass in this cycle. To do this, the biomass conversion efficiency is defined as the additional work obtained by the implementation of the recuperation cycle, divided by the energy released by the biomass combustion,

$$\eta_{BM} = \frac{W - W_c - W_p - N^{F1} LHV_{CH_4} \eta_E}{N^{BM} LHV_{BM}} \quad (13)$$

where W, W_c and W_p are again the engine, the compressor and the pump work respectively (kW), LHV_{CH_4} and LHV_{BM} are the lower heating values of methane and biomass (kJ/kmole), and N^{F1} and N^{BM} are their mole flow (kmole/s) and η_E is the engine brake efficiency, which is set at 40%. The definition of the biomass conversion assumes that no recuperation is feasible without the implementation of the secondary burner. This assumption is based on the results shown in the previous simulation. Fig. 12 shows that the proposed way of burning biomass is an efficient way to produce power.Indeed, it appears to be more efficient than any other biomass fuelled cycle currently in use, e.g. [45,62–65].

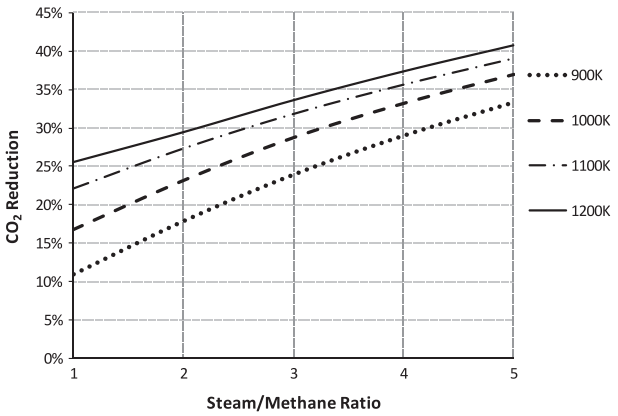

Fig. 11. Hybrid cycle CO_2 emissions reduction, relative to a 40% efficient natural gas engine, versus steam–methane ratio, for different SMR temperatures.

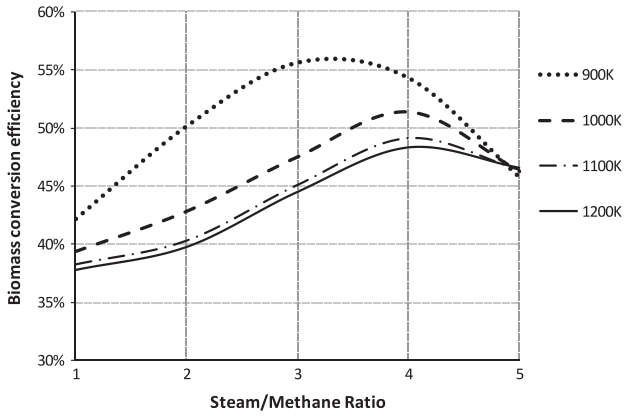

Fig. 12. Hybrid cycle biomass efficiency versus steam–methane ratio for the different SMR temperatures.

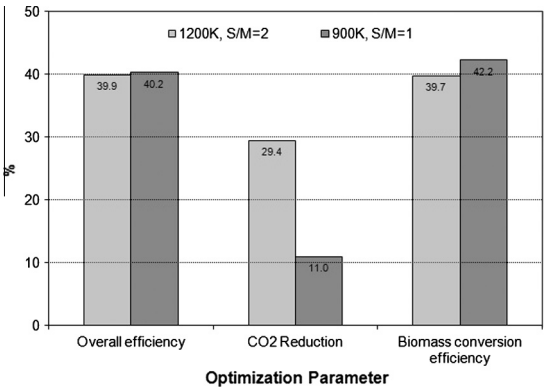

Fig. 14. Hybrid cycle overall efficiency, CO_2 reduction compared to a 40% efficient natural gas ICE and biomass conversion efficiency at different operating conditions.

4.2.2. Most feasible system configuration

A comparison of Figs. 8, 11 and 12 shows that the cycle's overall efficiency, CO_2 emissions and biomass conversion efficiency have different trends and are maximised at different operating conditions. Determination of optimal operating conditions therefore depends non-trivially on what metric is used to determine optimality.

Further, a significant assumption made in this work is that engine efficiency is not affected by steam content in the fuel. Whilst the effects of high steam content on the engine cannot be categorically stated without experimentation, numerous works in the literature have shown that significant levels of water addition in internal combustion engines can indeed sometimes improve engine performance although, of course, at some limit it must become a penalty [66,67]. Fig. 13 shows the mass fraction of water in the fuel mixture. Based on the literature, a limit on the steam mass fraction in the fuel of 30% is considered reasonable. It is emphasised that the equivalent steam mole fraction is significantly lower. This imposes a steam methane ratio of between 1 and 2, depending on the SMR temperature.

Fig. 14 shows the performance of two particular configurations that meet this restriction on steam–methane ratio. Whilst the overall efficiency and the biomass conversion efficiency of the cycle is slightly higher when running the SMR at 900 K and a steam/methane ratio of 1, the CO_2 emission reduction relative to an unrecuperated natural gas engine is greater when running the SMR at 1200 K and a steam/methane ratio of 2. Thus, whilst both may be technically feasible, determination of which is superior depends on the performance metric, which is likely to consider other parameters such as the cost of CO_2 emissions and the price and availability of biomass and natural gas.

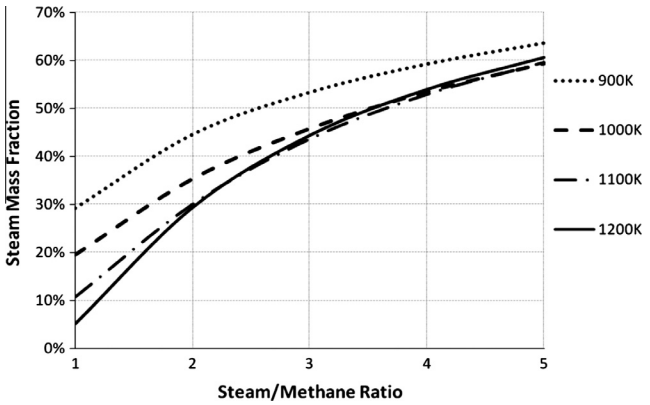

Fig. 13. Hybrid cycle mass fraction of steam leaving the SMR versus steam–methane ratio for the different SMR temperatures.

4.2.3. Effect of system size

Because engine efficiency increases with size, it is relevant to see its effect on the overall cycle, especially on its CO_2 emissions. Based on what was discussed in the previous section simulations were carried out incrementing the engine efficiency in 5% steps from 35% to 60%, while maintaining the other cycle parameters constant (Table 1). Although the actual maximum electrical efficiency for ICE generators is around 45–50% (e.g. [68]), higher engine efficiencies are evaluated as a projection.

Fig. 15 shows that for smaller engines, with efficiencies of up to roughly 35%, the biomass efficiency and the overall efficiency of the cycle match that of the engine. This is because as the efficiency of the engine drops there is more enthalpy available in the exhaust and therefore the recuperation stage works better. This is also evident when examining the biomass–methane energy ratio, which shows that as the engine efficiency drops less biomass is needed. The opposite effect is seen for big engines, were efficiencies are higher. In this case the lack of enthalpy in the exhaust has to be overcome by the burning of more biomass. Comparing Fig. 15a and b it can be seen that the biomass–methane ratio of the power plant is strongly related to the SMR temperature.

Fig. 16 shows the CO_2 produced by the cycle and the reduction obtained when compared to those of a 58% efficient natural gas combined cycle (NGCC), which emits 370 $gCO_2/kW\,h$ and is roughly the state-of-the-art for such devices. It shows that the CO_2 reductions are strongly related to the SMR temperature. Further, it can be seen that if the cycle is used on small engines (i.e. with lower efficiencies) it produces likely more $CO_2/kW\,h$ than a NGCC, depending on the SMR temperature. However, as the plant gets bigger and the engine efficiency is increased, the proposed cycle produces less CO_2 than the NGCC, achieving a potential 19% saving at an engine efficiency of 50%.

However, in order to have a more precise idea of the viability of the proposed cycle, an economic analysis needs to be done. This is addressed in the second part of this work.

5. Conclusions

This paper presented a thermodynamic analysis of two chemically recuperated, internal combustion engine (ICE) driven generating plants. This analysis was conducted using ASPEN+.

The first plant featured a methane fuelled ICE with chemical recuperation. The analysis examined varying engine coolant loads

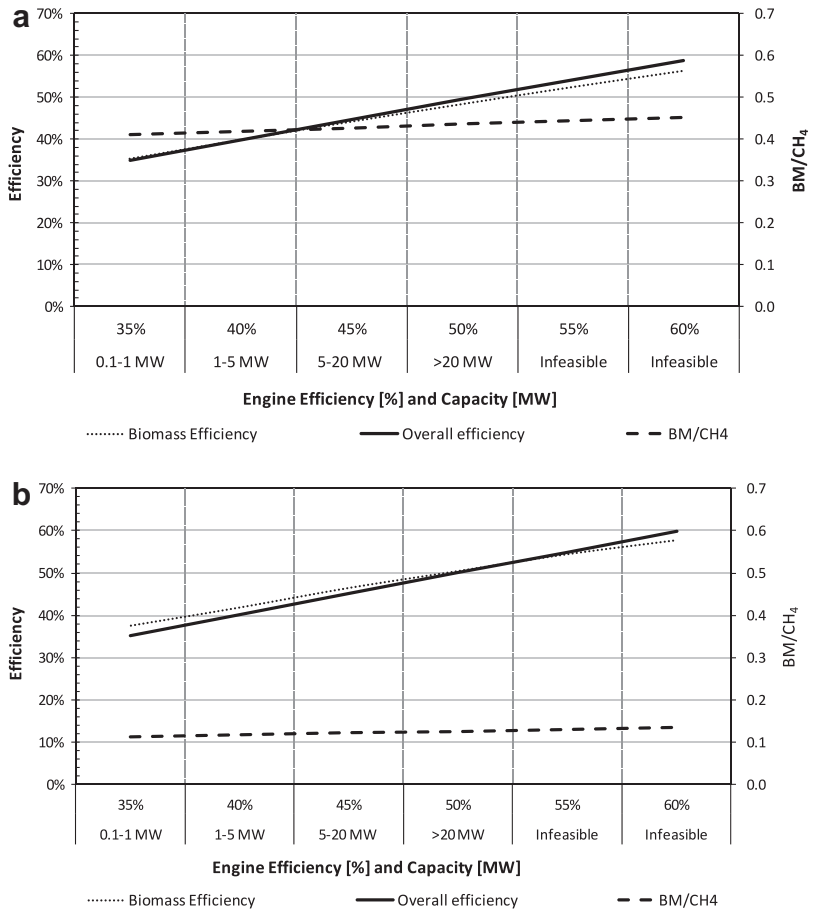

Fig. 15. Hybrid cycle overall efficiency, biomass efficiency and biomass-CH_4 ratio versus engine efficiency and nominal capacity at the cycle operating conditions shown on Table 1. (a) Steam–methane ratio = 2 and SMR temperature of 1200 K. (b) Steam–methane ratio = 1 and SMR temperature of 900 K.

and steam–methane ratios, and the following observations were made.

1. When running the engine at $\lambda = 2$ and at normal engine coolant loads (30–30% exhaust-cooling enthalpy split, with the remaining 40% of the fuel's energy becoming engine brake work), the chemical recuperation is unlikely to be feasible for any of the steam–methane ratios evaluated, as none of them achieve a reformer temperature greater than 700 K, which is considered the lower practical limit for steam–methane reforming.
2. In order for the plant to be marginally more efficient that an equivalent, conventional, non-recuperated ICE, roughly a 45–15% exhaust-cooling enthalpy split needs to be achieved. In this case, the efficiency improvement is due to both chemical and heat recuperation.
3. The added engine efficiency when increasing the steam–methane ratio, while keeping the exhaust-cooling enthalpy split constant, was mainly due to heat recovery and not chemical recuperation.

Thus, it is unlikely that this system will be attractive because of its added complexity and modest potential improvements in overall efficiency relative to a conventional natural gas engine plant.

The second plant analysed was a so-called hybrid, and used both methane and biomass fuels. This plant boosted the energy available for chemical recuperation by using the biomass combustion products to heat the reformer. The following observations were made.

1. The overall efficiency of the plant, when defined in terms of the heating values of both the methane and biomass, was similar to the conventional, methane fuelled engine.
2. However, the efficiency of the conversion of the biomass fuel energy to work output appears to be higher than for other biomass fuelled technologies currently in use. This is achieved whilst not passing the biomass combustion products through the engine, which should yield other benefits related to improved engine reliability.
3. Further, in the ideal limit of a fully renewable biomass fuel, the burning of biomass does not contribute to the net CO_2 emissions, and the CO_2 emission reduction for this second plant can be significant.

Indeed, an implementation of the second plant using larger ICE's, which have efficiencies of around 45–50%, could result in CO_2 emission reductions of around 10–20% when compared to those of a natural gas combined cycle power station. This is a significant result, since NGCCs are commonly considered to have the lowest CO_2 emissions of all forms of fossil fuelled, power generation currently in use.

Thus, the hybrid nature of this second plant appears to combine attractive aspects of the fossil and renewable fuels. The plant may enable more efficient conversion of the biomass fuel's energy than has been achieved for biomass fuelled plants to date by exploiting the high efficiency of the integrated plant. Further, CO_2 emissions of the overall plant are low because of the biomass fuel. The next part of this study [69] will therefore examine the economics of this proposed hybrid plant.

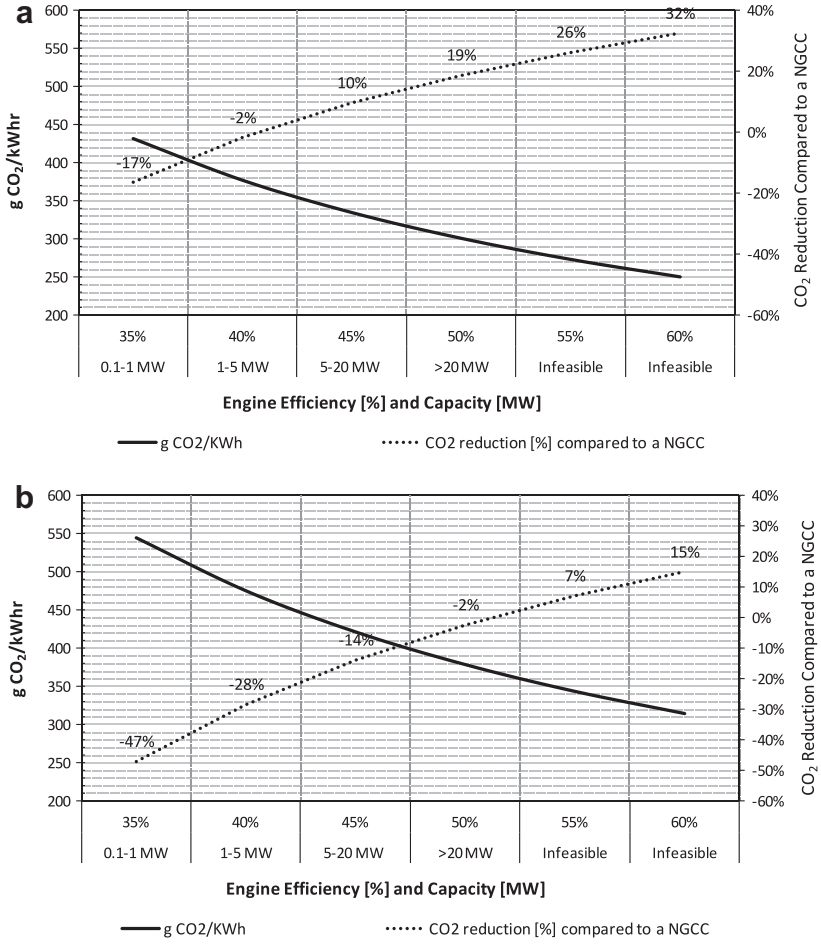

Fig. 16. Hybrid cycle gCO_2/kW h and CO_2 reduction relative to a NGCC versus engine efficiency and nominal capacity at the cycle operating conditions shown on Table 1. (a) Steam–methane ratio = 2 and SMR temperature of 1200 K. (b) Steam–methane ratio = 1 and SMR temperature of 900 K.

References

[1] Udomsri SN, Martin AR, Fransson TH. Economic assessment and energy model scenarios of municipal solid waste incineration and gas turbine hybrid dual-fueled cycles in thailand. Waste Manage 2010;30:1414–22.

[2] Sik Pak P, Kosugi T. Characteristics and economic evaluation of CO_2-capturing power generation systems using solar thermal energy and gasified coal. Electr Eng Jpn 2002;138.

[3] Baghernejad A, Yaghoubi M. Exergoeconomic analysis and optimization of an integrated solar combined cycle system (ISCCS) using genetic algorithm. Energy Convers Manag 2011;52:2193–203.

[4] Pihl E, Heyne S, Thunman H, Johnsson F. Highly efficient electricity generation from biomass by integration and hybridization with combined cycle gas turbine (CCGT) plants for natural gas. Energy 2010;35:4042–52.

[5] Montes MJ, Rovira A, Muñoz M, Martínez-Val JM. Performance analysis of an integrated solar combined cycle using direct steam generation in parabolic trough collectors. Appl Energy 2010;88:3228–38.

[6] Behara O, Kellafb A, Mohamedia K, Belhamelb M. Instantaneous performance of the first integrated solar combined cycle system in algeria. Energy Procedia 2011;6:185–93.

[7] Kucukvar M, Tatari O. A comprehensive life cycle analysis of cofiring algae in a coal power plant as a solution for achieving sustainable energy. Energy 2011;36:6352–7.

[8] Marchetti JM, Errazu AF. Technoeconomic study of supercritical biodiesel production plant. Energy Convers Manage 2008;49(8):2160–4.

[9] Essalaimeh S, Al-Salaymeh A, Abdullat Y. Electrical production for domestic and industrial applications using hybrid pv-wind system. Energy Convers Manage 2013;65(SI):736–43.

[10] Tsagarakis Konstantinos P. Optimal number of energy generators for biogas utilization in wastewater treatment facility. Energy Convers Manage 2007;48(10):2694–8.

[11] Esen Hikmet, Inalli Mustafa, Esen Mehmet. Technoeconomic appraisal of a ground source heat pump system for a heating season in eastern turkey. Energy Convers Manage 2006;47:1281–97.

[12] Aspen Technology, Inc. Aspen Plus. http://www.aspentech.com.

[13] Elshout Ray. Hydrogen production by steam reforming. Chem Eng 2010;117(5):34–8.

[14] Grace JR, Li X, Jim Lim C. Equilibrium modelling of catalytic steam reforming of methane in membrane reactors with oxygen addition. Catal Today 2001;64:141–9.

[15] Yu W, Ohmori T, Yamamoto T, Endo A, Nakaiwa M, Itoh N. Optimal design and operation of methane steam reforming in a porous ceramic membrane reactor for hydrogen production. Chem Eng Sci 2007;62:5627–31.

[16] Rosen MA. Thermodynamic comparison of hydrogen production processes. Int J Hydrogen Energy 1996;21:349–65.

[17] Simpson AP, Lutz AE. Exergy analysis of hydrogen production via steam methane reforming. Int J Hydrogen Energy 2007;32:4811–20.

[18] Hou K, Hughes R. The kinetics of methane steam reforming over a $Ni/\alpha - Al_2O$ catalyst. Chem Eng J 2001;82(1-3):311–28.

[19] Akers WW, Camp DP. Kinetics of the methane steam reforming. AIChE J 1955.

[20] Allen DW, Gerhard ER, Likins Jr MR. Kinetics of the methane steam reaction. Ind Eng Chem Proc Des Dev 1975.

[21] Al-Ubaid AS, Elnashaie SSEH, Abashar M. Methane conversion. New York.: Elsevier; 1988.

[22] Rostrup-Nielsen JR. Catalysis. Sci Technol 1984;5:3.

[23] Matsumura Y, Nakamori T. Steam reforming of methane over nickel catalysts at low reaction temperature. Appl Catal 2004;258(1):107–14.

[24] Olmsted JH, Grimes PG. Heat engine efficiency enhancement through chemical recovery of waste heat. In: Proceedings of 7th international energy conversion engineering conference; 1972.

[25] Rostrup-Nielsen JR. Steam reforming and chemical recuperation. Catal Today 2009;145:72–5.

[26] Verkhivker G, Kravchenko V. The use of chemical recuperation of heat in a power plant. Energy 2004;29:379–88.

[27] Lloyd A. Thermodynamics of chemically recuperated gas turbines. Master's thesis, center for energy and environmental studies, Princeton University, USA; 1991.

[28] Selimovic A, Palson J, Sjunneson L. Fuel cell seminar, palm springs; 1991. p. 88.

[29] Harvey S, Kane N. Analysis of a reheat gas turbine cycle with chemical recuperation using Aspen+. Energy Convers Manage 1997;38:1671–9.

[30] Abdallah H, Harvey S. Thermodynamic analysis of chemically recuperated gas turbines. Int J Therm Sci 2001;40:372–84.
[31] Janes J. Chemically recuperated gas turbine, final report. Technical report, California Energy Commission; 1990.
[32] Johannes E, Li X, Neels J, Towgood Pl. Transient performance of a non-catalytic syngas generator for active DPF regeneration and NOx reduction. SAE Technical Papers, 2008-01-0446(2008-01-0446); 2008.
[33] Chakravarthy VK, Daw CS, Pihl JA, Conklin JC. Study of the theoretical potential of thermochemical exhaust heat recuperation for internal combustion engines. Energy Fuels 2010;24:1529–37.
[34] Søogaard C, Schramm J, Jensen TK. Reduction of UHC emissions from natural gas fired SI-engine-production and application of steam reformed natural gas, SAE Technical Papers, 2000-01-2823(2000-01-2823); 2000.
[35] Posada F, Bedick C, Clark NN, Kozlov A, Linck M, Boulanov D, et al. Low-temperature combustion with thermo-chemical recuperation. SAE Technical Papers, 2007-01-4074(2007-01-4074); 2007.
[36] Shimada A, Ishikawa T. Improvement of thermal efficiency using fuel reforming in SI engine. SAE Technical Papers, 2010-01-0584(2010-01-0584); 2010.
[37] Ma F, Wang Y, Liu H, Wang J, Li Y, Zhao S. Experimental study on thermal efficiency and emission characteristics of a lean burn hydrogen enriched natural gas engine. Int J Hydrogen Energy 2007;32:5067–75.
[38] Karim GA, Wierzba I, Al-alousi Y. Methane–hydrogen mixtures as fuels. Int J Hydrogen Energy 1996;21:625–31.
[39] Dimopoulos P, Boulouchos K, Rechsteiner C, Soltic P, Hotz R. Combustion characteristics of hydrogen–natural gas mixtures in passenger car engines. SAE Technical Papers, 2007-24-0065(2007-24-0065); 2007.
[40] Tunestal P, Christensen M, Einewall P, Andersson T, Johansson B, Jonsson O. Hydrogen addition for improved lean burn capability of slow and fast burning natural gas combustion chambers. SAE Technical Papers, 2002-01-2686(2002-01-2686); 2002.
[41] Thurnheer T, Soltic P, Eggenschwiler PD. S.I. engine fuelled with gasoline methane and methane/hydrogen blends: heat release and loss analysis. Int J Hydrogen Energy 2009;34(5):2494–503.
[42] Ma F, Liu H, Wang Y, Li Y, Wang J, Zhao S. Combustion and emission characteristics of a port-injection HCNG engine under various ignition timings. Int J Hydrogen Energy 2008;33:816–22.
[43] Gamiño B, Aguillón J. Numerical simulation of syngas combustion with a multi-spark ignition system in a diesel engine adapted to work at the otto cycle. Fuel 2010;89:581–91.
[44] Gamiño B, Aguillón J. Numerical simulation of syngas combustion with a multi-spark ignition system in a diesel engine adapted to work at the otto cycle. Fuel 2010;89:581–91.
[45] Cohce MK, Dincer I, Rosen MA. Thermodynamic analysis of hydrogen production from biomass gasification. Int J Hydrogen Energy 2010;35:4970–80.
[46] Stolarski M, Krzyzaniak M, Graban L. Evaluation of energy-related and economic aspects of heating a family house with dendromass in the north-east of poland. Energy Build 2011;43:433–9.
[47] Yin C. Prediction of higher heating values of biomass from proximate and ultimate analyses. Fuel 2011;90:1128–32.
[48] Chen Z, Yan Y, Elnashaie SSEH. Novel circulating fast fluidized-bed membrane reformer for efficient production of hydrogen from steam reforming of methane. Chem Eng Sci 2003;58:4335–49.
[49] Dyer PN, Chen CM. Engineering development of ceramic membrane reactor system for converting natural gas to H_2 and syngas for liquid transportation fuel. Technical report, Proceedings of the 1999 hydrogen program review, DOE.
[50] Makel D. Low cost microchannel reformer for hydrogen production from natural gas. Technical report, California Energy Commission (CEG), Energy Innovations Small Grant (EISG) Program.
[51] Mleczko L, Ostrowski T, Wurzel T. A fluidised-bed membrane reactor for the catalytic partial oxidation of methane to synthesis gas. Chem Eng Sci 1996;51:3187–92.
[52] Adris AM, Lim CJ, Grace JR. The fluidized bed membrane reactor system: a pilot scale experimental study. Chem Eng Sci 1994;49:5833–43.
[53] Abbasi Atibeh Payman, Dennis Peter A, Orbaiz Pedro J, Brear Michael J, Watson Harry C. Lean burn performance of a natural gas fuelled, port injected, spark ignition engine, 04 2012.
[54] Abbasi Atibeh P, Dennis PA, Orbaiz PJ, Brear MJ, Watson HC. Lean limit combustion analysis for a spark ignition natural gas internal combustion engine. Combust Sci Technol 2013;185(8):1151–68. http://dx.doi.org/10.1080/00102202.2013.769785.
[55] Verhelst S, Wallner T. Hydrogen-fueled internal combustion engines. Prog Energy Combust Sci 2009;35:490–527.
[56] Verhelst S, Sierens R, Verstraeten S. A critical review of experimental research on hydrogen fueled SI engines. SAE Paper 2006-01-0430; 2006.
[57] Herdin G. Hydrogen and hydrogen mixtures as fuel in stationary gas engines. SAE Technical Papers, 2007-01-0012(2007-01-0012); 2007.
[58] Einewall P, Tunestal P, Johansson B. Lean burn natural gas operation vs. stoichiometric operation with EGR and a three way catalyst. SAE Technical Papers, (2005-01-0250); 2005.
[59] Ibrahim A, Bari S. A comparison between EGR and lean-burn strategies employed in a natural gas SI engine using a two-zone combustion model. Energy Convers Manage 2009;50(12):3129–39.
[60] Semin RAB. A technical review of compressed natural gas as an alternative fuel for internal combustion engines. Am J Eng Appl Sci 2008;1(4):302–11.
[61] Abbasi Atibeh P. Performance of a spark ignition, lean burn, natural gas internal combustion engine. Master's thesis, Department of Mechanical Engineering, The University of Melbourne; 2012.
[62] Cohce MK, Rosen MA, Dincer I. Efficiency evaluation of a biomass gasification-based hydrogen production. Int J Hydrogen Energy 2011;36:11388–98.
[63] Vitasari CR, Jurascik M, Ptasinski KJ. Exergy analysis of biomass-to-synthetic natural gas (SNG) process via indirect gasification of various biomass feedstock. Energy 2011;36:3825–37.
[64] Hutchinson J. Program on technology innovation: integrated generation technology options. Technical report, EPRI, June 2011.
[65] Tiangco V, Sethi P, Zhang Z. Biomass strategic value analysis. Technical report, Energy Research and Development Division California Energy Commission, 2005.
[66] Dryer FL. Water addition to practical combustion systems-concepts and applications. Sym (Int) Combust 1977;16(1):279–95.
[67] Subramanian V, Mallikarjuna JM, Ramesh A. Effect of water injection and spark timing on the nitric oxide emission and combustion parameters of a hydrogen fuelled spark ignition engine. Int J Hydrogen Energy 2007;32:1159–73.
[68] Wartsila. Power plants product catalogue; 2011.
[69] Orbaiz PJ, Brear MJ. A technical and financial analysis of two chemically recuperated, reciprocating engine driven power plants. Part 2: financial analysis. Energy Convers Manage, 2013 [in press].